

# Copolymerization of $\epsilon$ -Caprolactone with (3*S*)-3-[(Benzyloxycarbonyl)methyl]morpholine-2,5-dione and the $^{13}\text{C}$ NMR Sequence Analysis of the Copolymer

Dong Wang and Xin-De Feng\*

Department of Polymer Science and Engineering, Peking University, 100871 Beijing, China

Received October 2, 1997; Revised Manuscript Received March 4, 1998

**ABSTRACT:** (3*S*)-3-[(Benzyloxycarbonyl)methyl]morpholine-2,5-dione (BMD) has been successfully copolymerized with  $\epsilon$ -caprolactone for a wide range of mole fractions in the feed. The sequence analysis of the copolymers has also been carried out on the basis of the clear interpretation of the  $^{13}\text{C}$  NMR spectra of the copolymers. DCA (dynamic contact angle) measurements for the deprotected copolymers show that the biodegradable polymers possess good hydrophilicities.

## Introduction

The homo- and copolymers of lactide and lactone such as polylactide, poly(lactide-*co*-glycolide) and poly( $\epsilon$ -caprolactone-*co*-lactide) are among well-known biodegradable synthetic polymers which have been studied for many years.<sup>1</sup> Due to their excellent behavior *in vivo*, they are widely used in biorelated fields.

Our laboratory had reported the living polymerization of lactide and  $\epsilon$ -caprolactone using Al/Zn bimetallic initiator.<sup>2,3</sup> The above diblock copolymers with a certain block ratio can provide a zero-order release rate for hydrophobic drugs like Norgestrel,<sup>4</sup> but they are not suitable for water-soluble drugs. The hydrophobic nature of polyesters can lead to lower drug loading and can cause trouble in microencapsulation processes used for drug delivery systems.<sup>5,6</sup>

In order to improve the hydrophilicity of these polyesters, one may introduce hydrophilic pendant functional groups into the polymer chain.<sup>7–14</sup> Feijen et al.<sup>13</sup> reported the copolymerization of  $\epsilon$ -caprolactone and morpholine-2,5-dione with pendant hydrophilic functional group (MDP) using stannous octoate as catalyst. However, they failed to achieve copolymers with a content of MDP exceeding 20%. The lysine  $\epsilon$ -amino groups in linear poly(L-lactic acid-*co*-L-lysine) copolymers with about 1% lysine content have been utilized to initiate the ring opening polymerization of the amino acid *N*-carboxyanhydrides to yield the comblike graft copolymer.<sup>15</sup> However, the reaction process is very complicated. Ouchi et al.<sup>16,17</sup> reported the synthesis of cyclo[Asp(OBzl)-Glc]. It was homopolymerized in bulk using stannous octoate as catalyst. The  $\bar{M}_n$  of the resulting poly[Asp(OBzl)-alt-Glc] ranges from 1950 to 3280.

Recently, we reported the synthesis of the same monomer, (3*S*)-3-[(benzyloxycarbonyl)methyl]morpholine-2,5-dione (BMD).<sup>18</sup> The homopolymerization of the monomer was successfully carried out using stannous octoate as catalyst. The  $\bar{M}_n$  values of the polymers range from 5800 to 13500. The FTIR spectrum of our monomer is rather different from that of Ouchi's in the position of the N–H stretch. It comes at  $3196\text{ cm}^{-1}$  in our work, while in Ouchi's papers it appears at  $3358\text{ cm}^{-1}$ . This difference may indicate the existence of different association forms of the monomer on the basis

of the hydrogen bond. The association form in our monomer to a certain extent may prevent –NH– from contacting the catalyst, which may interfere with the polymerization process. The validation of the above analysis, however, requires single crystal data for the monomer.

In the present work, we copolymerized  $\epsilon$ -caprolactone and BMD with large variations of mole fraction in the feed. The benzyl protective group in the copolymers was eliminated by catalytic hydrogenation. The interpretations of  $^{13}\text{C}$  NMR spectra of the copolymers and the sequence analysis of them based on these interpretations are also described in detail. The hydrophilicity of the resulting deprotected copolymers is characterized by dynamic contact angle (DCA).

## Experimental Section

**Materials.** Stannous octoate was purchased from Aldrich and was used as received.  $\epsilon$ -Caprolactone was purchased from Aldrich and distilled from  $\text{CaH}_2$  under reduced pressure just before use. (3*S*)-3-[(Benzyloxycarbonyl)methyl]morpholine-2,5-dione (BMD) was prepared as described previously.<sup>18</sup> Tetrahydrofuran (THF) was distilled from  $\text{CaH}_2$ . All of the other reagents were purchased from Beijing Chemical Reagent Co. and used without further purification.

**Methods.** Melting points were measured with the Thiele apparatus.

Elemental analyses were carried out by the Center of Analysis & Testing of Peking University.

$^1\text{H}$  NMR and  $^{13}\text{C}$  NMR spectral studies were performed on a Bruker ARX-400 spectrometer. Tetramethylsilane was used as an internal standard.

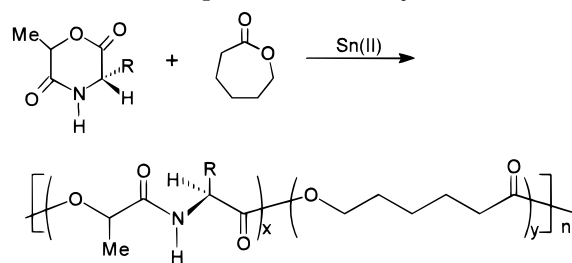
Mass spectra were obtained with a VG ZAB-HS mass spectrometer (EI).

FTIR results were obtained from a Nicolet Magna-IR 750 spectrometer.

The  $\bar{M}_n$  and  $\bar{M}_w$  of the copolymers were determined by gel permeation chromatography (GPC). The GPC measurements were carried out with THF as eluent (1.0 ml/min) using a Waters 510 pump, a Waters U6K injector, three Waters  $\mu$ Styragel columns ( $10^5$ ,  $10^4$ , and  $500\text{ \AA}$ ) in series, and a Waters 401 differential refractometer. The columns were calibrated with polystyrene standards having a narrow molecular weight distribution.

Dynamic contact angles of the deprotected copolymers were tested by a CAHN dynamic contact angle analyzer (DCA-322) at  $37^\circ\text{C}$  in distilled water.

The DCA samples were prepared according to the following process. Polymer samples were dissolved in DMSO (2%, w/w).

**Scheme 1. Copolymerization of MDP and CL Reported Previously**

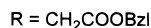
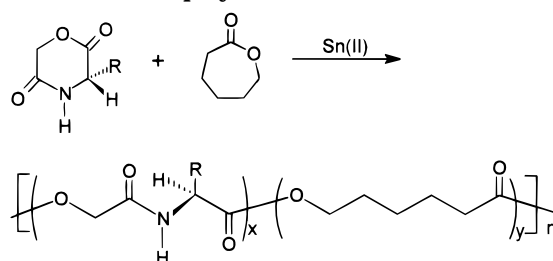
A long cover glass was dipped into the solution and lifted at a constant speed to allow a thin film of the polymer to form evenly on the surface of the glass. The samples were air-dried for 3 days and treated in vacuo for another 6 h at room temperature to eliminate any remaining solvent.

**Polymerization.** The polymerization tubes were silanized and kept at 110 °C for 24 h. A specific amount of BMD and a dry stirring bar were put into the warm tube quickly. Then it was dried in vacuo for 8 h at 56 °C and sealed with a dry rubber septum. The tube was connected to the Schlenk line, where exhausting–refilling with dry  $\text{N}_2$  was repeated 3 times. The BMD in the tube melted completely after the tube was put into an oil bath (155 °C). Soon afterward, newly distilled  $\epsilon$ -caprolactone was added into the sealed tube with a dry syringe. With vigorous stirring, a specific amount of stannous octoate in dry toluene (0.2 M) was added into the mixture. Five minutes later, the exhausting–refilling process was carried out again to remove the toluene. After the addition of catalyst, the temperature of the oil bath was lowered to  $152 \pm 1$  °C. When the polymerization was finished, the reaction was stopped by putting the tube into the freezer. The tube was broken, and the resulting product was dissolved in THF and dropped into excess petroleum ether (30–60 °C). The precipitate was filtered and dried in vacuo at 56 °C for 6 h. After a small amount of the solid was saved for NMR studies, the remaining product was dissolved in THF again and precipitated with excess methanol to remove the monomer. The copolymer was dried in vacuo at 56 °C for another 6 h to eliminate solvents which may interfere with the  $^1\text{H}$  NMR and  $^{13}\text{C}$  NMR spectra of the copolymer.

**Deprotection of the Copolymer.** The resulting copolymer was dissolved in 20 mL of THF. Methanol (6 mL) was added to the solution, accompanied by a small amount of Pd/C (5%) suspended in methanol. With vigorous stirring, hydrogen gas was bubbled through the suspension for 60 h. After the removal of the Pd/C powder, the solution was dropped into excess petroleum ether (30–60 °C). The precipitate was dried in vacuo at 56 °C for 6 h.

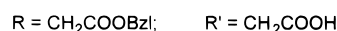
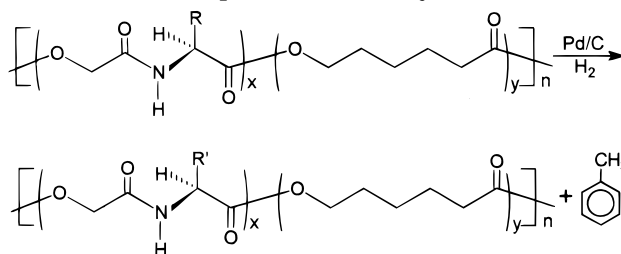
## Results and Discussion

**Copolymerization.** The copolymerization of  $\epsilon$ -caprolactone and morpholine-2,5-dione derivatives with a pendant functional group (MDP) had been reported previously<sup>13</sup> (Scheme 1). The content of MDP in the copolymers was less than 20%. Their work also revealed that the reactivity of the monomer would decrease with the increase of number and size of the substitute group on the morpholine ring. Taking this into account, we synthesized (3*S*)-3-[(benzyloxycarbonyl)methyl]morpholine-2,5-dione (BMD), which has no substitute group on the 6-position of the morpholine ring. The high reactivity of the monomer has been proved by its successful homopolymerization reported in our earlier work.<sup>18</sup> In the present paper, we copolymerized  $\epsilon$ -caprolactone and BMD (Scheme 2), with the mole fraction of BMD ranging from 0.093 to 0.897.

**Scheme 2. Copolymerization of BMD and CL****Table 1. Results of Copolymerization of  $\epsilon$ -Caprolactone and BMD<sup>a</sup>**

sample no.	$x_B^b$	$X_B^b$	% convn		yield (%)	$10^{-4} \bar{M}_n$	$10^{-4} \bar{M}_n$	$\bar{M}_w/\bar{M}_n$
			BMD <sup>b</sup>	CL <sup>b</sup>				
1	0.093	0.093	100	100	98.3	4.30	13.24	3.08
2	0.194	0.194	100	100	95.0	1.97	7.23	3.66
3	0.517	0.495	95.5	95.0	85.6	0.66	2.77	4.18
4	0.753	0.730	91.1	88.0	83.2	0.79	2.14	2.73
5	0.897	0.877	82.6	82.3	76.5	0.58	1.96	3.40

<sup>a</sup>  $t = 250$  min; mole ratio monomer/catalyst = 1000/1. <sup>b</sup>  $x_B$  is the mole fraction of BMD in feed;  $X_B$  is the mole fraction of BMD in copolymer.  $x_B$ ,  $X_B$ , and conversion of monomers are calculated from the data of  $^1\text{H}$  NMR spectrum ( $\text{CDCl}_3$ ).

**Scheme 3. Deprotection of Poly(CL-*co*-BMD)**

The polymerization was performed in bulk using stannous octoate as catalyst, and the results of copolymerization were listed in Table 1. It is seen that the newly synthesized monomer has higher reactivity than the reported monomers which bear substitute on the 6-position of the morpholine ring.<sup>13,14</sup> The conversion of BMD is high (over 80% when  $x_B$  is 0.897). On the other hand, the conversions of CL are not always very high for different mole fractions in the feed, as expected. The molecular weight of the copolymer would decrease while  $x_B$  increases with a decrease of the overall yield of the copolymers. Since broad MWD was always observed, the possibility of a severe transesterification reaction is great.

**Deprotection of Poly(CL-*co*-BMD).** It was reported that the benzyl protective group of the pendant carboxylic acid could be removed by catalytic hydrogenation using Pd/C as catalyst.<sup>19</sup> In the present work, we used the same method to remove the benzyl protective group in poly(CL-*co*-BMD) (Scheme 3).

Compared with the  $^1\text{H}$  NMR spectrum of the protected copolymer, the peaks around 5.1 and 7.3 ppm which are assigned to the hydrogen atoms of the BzI protected group almost disappear in the spectrum of the deprotected copolymer after 60 h of hydrogenation (Figure 1). This clearly demonstrates the effectiveness of the deprotection method. However, the data from the

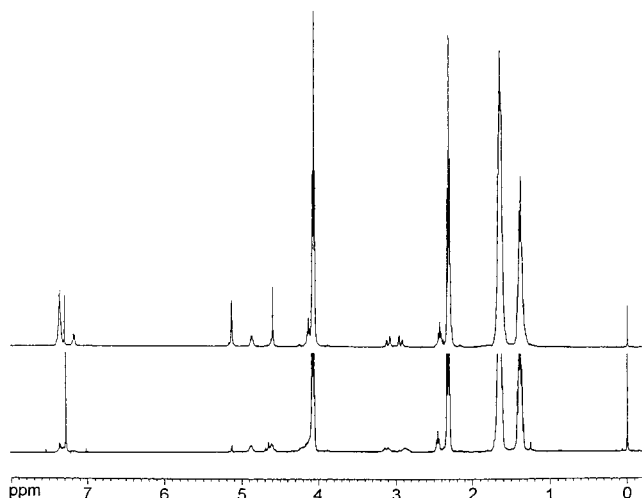


**Figure 1.**  $^1\text{H}$  NMR spectrum ( $\text{CDCl}_3$ ) of protected (upper) and deprotected (lower) copolymers ( $X_B = 0.093$ ).

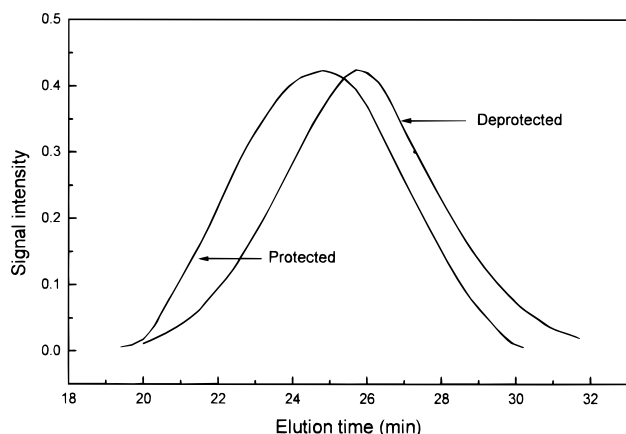


**Figure 2.** GPC trace of both protected and deprotected copolymer ( $X_B = 0.093$ ).

$^1\text{H}$  NMR spectrum also reveal that still less than 20% of the Bzl group remains unmoved. This is mainly due to the higher molecular weight of the selected sample (no. 1 in Table 1) which may trap the Bzl group and prevent it from contacting the Pd/C powder.

The GPC trace of both the protected copolymer and the deprotected copolymer (no. 1) is shown in Figure 2. It reveals a reduction of  $\bar{M}_n$  from 43 000 to 26 500 after the deprotection process. The MWD is also broadened from 3.08 to 3.6. This change can be attributed to the elimination of the Bzl protective group and the unnecessary main chain cleavage at the aliphatic ester bonds in the deprotection process.

**Sequence Analysis.** Obviously, the properties of the deprotected copolymers including their hydrophilicity and their performance in producing drug delivering systems are closely related to the sequence distribution of the two components in the copolymers. The following analysis of the sequence was worked out on the basis of the NMR spectrum of poly(CL-co-BMD). Because the deprotection method used in this work does not change the sequence of the copolymer chain, the results stated below can also be used to describe the sequence distribution of the deprotected copolymers.

Both  $^1\text{H}$  NMR and  $^{13}\text{C}$  NMR spectroscopy are considered in the sequence analysis of poly(CL-co-BMD).  $^{13}\text{C}$  NMR spectroscopy has been proved to be an effective

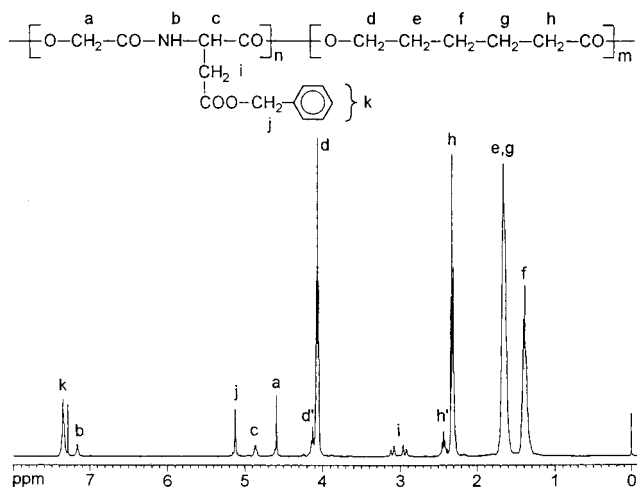


**Figure 3.**  $^1\text{H}$  NMR spectrum ( $\text{CDCl}_3$ ) of poly(CL-co-BMD) ( $X_B = 0.093$ ).

method in the sequence analysis of polyesters, polyamides, and polyesteramides<sup>20–22</sup> while  $^1\text{H}$  NMR spectroscopy is seldom used in these sequence analyses.

By comparison with  $^1\text{H}$  NMR spectra of PCL<sup>23</sup> and PBMD (Figure 5), each group of peaks in the  $^1\text{H}$  NMR spectrum of poly(CL-co-BMD) (Figure 3) are assigned as follows. Chemical shifts in  $^1\text{H}$  NMR:  $\delta$  (ppm) = 1.2399–1.4319 ( $\text{H}_f$ ), 1.6158–1.6916 ( $\text{H}_{e,g}$ ), 2.2932–2.4253 ( $\text{H}_h$ ), 2.9521–3.0799 ( $\text{H}_i$ ), 4.0448–4.1405 ( $\text{H}_d$ ), 4.5852 ( $\text{H}_a$ ), 4.8510–4.8707 ( $\text{H}_c$ ), 5.1220–5.1261 ( $\text{H}_j$ ), 7.1515–7.1710 ( $\text{H}_b$ ), 7.2857 ( $\text{CDCl}_3$ ), 7.3445–7.3879 ( $\text{H}_k$ ).

Among these peaks, both  $\text{H}_d$  and  $\text{H}_h$  show diad sensitivity, while  $\text{H}_e$ ,  $\text{H}_g$ , and  $\text{H}_f$  are insensitive to the sequence effect.  $\text{H}_h$  appears to be sensitive to the comonomer unit coupled to the carbonyl group but fails to give a response to the comonomer unit attached to the  $\epsilon$ -oxygen atom on the other side of the  $\epsilon$ -oxycaproyl unit (C). Peaks h are assigned to the  $\alpha$ -methylene proton which is connected to the C unit (C–C sequence). Peaks h are assigned to those coupled with (3S)-3-[(benzyloxycarbonyl)methyl]morpholine-2,5-dione unit (B) in the sequence C–B;  $\text{H}_a$  is only sensitive to the unit coupled to the  $\epsilon$ -oxygen atom. Peaks d and d' are assigned to the  $-\text{OCH}_2-$  proton in the C–C and B–C sequences, respectively. Unlike  $\text{H}_d$  and  $\text{H}_h$ , none of the proton in B unit shows sensitivity to the sequence effect, and it prevents us from detecting the existence of the B–B sequence. Because h–h' and d–d' are overlapping peaks from which it is difficult to obtain the correct integral ratio, they are no longer used in the sequence analysis of poly(CL-co-BMD).

The  $^{13}\text{C}$  NMR spectrum of the copolymer is shown in Figure 4. By use of the data from ref 23, peaks p–u of the  $\epsilon$ -oxycaproyl unit (C) are clearly determined. Chemical shifts in  $^{13}\text{C}$  NMR:  $\delta$  (ppm) = 24.3245–24.5564 ( $\text{C}_r$ ), 25.1485–25.5095 ( $\text{C}_s$ ), 28.0320–28.3289 ( $\text{C}_q$ ), 33.6687–34.1010 ( $\text{C}_l$ ), 64.0425–64.1273 ( $\text{C}_p$ ), 173.437–173.529 ( $\text{C}_u$ ). Although the  $^{13}\text{C}$  NMR data for PBMD have been reported by Ouchi et al.,<sup>16,17</sup> the different  $^{13}\text{C}$  NMR data in these two papers makes the assignment of carbon atoms in the B unit difficult. Fortunately, the assignments of each peak in the  $^1\text{H}$  NMR spectrum of PBMD (Figure 5) are clear. Chemical shifts in  $^1\text{H}$  NMR:  $\delta$  (ppm) = 2.980–3.021 ( $\text{H}_i$ ), 4.575–4.599 ( $\text{H}_a$ ), 4.725 ( $\text{H}_c$ ), 5.084 ( $\text{H}_j$ ), 7.288–7.321 ( $\text{H}_k$ ), 8.026 ( $\text{H}_b$ ). The two-

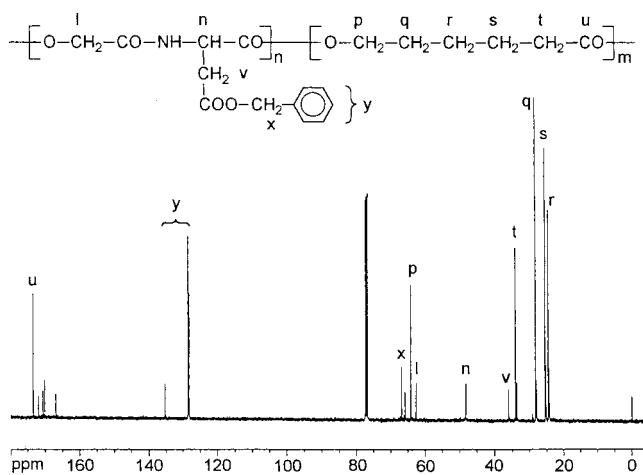


**Figure 4.**  $^{13}\text{C}$  NMR spectrum ( $\text{CDCl}_3$ ) of poly(CL-co-BMD) ( $X_B = 0.194$ ).

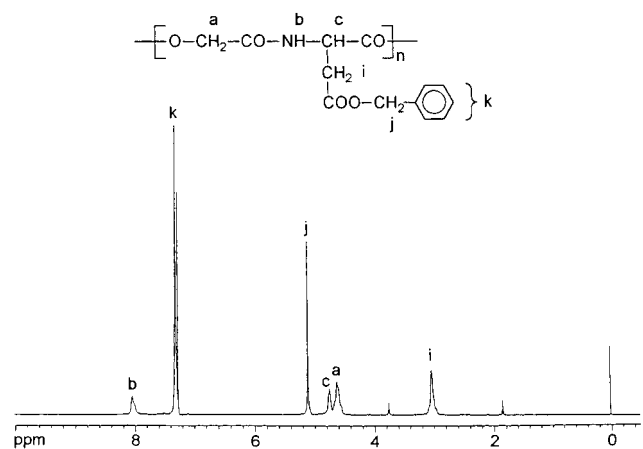


**Figure 5.**  $^1\text{H}$  NMR spectrum ( $\text{CDCl}_3$ ) of PBMD.

dimensional carbon–proton correlation with  $^{13}\text{C}$  and  $^1\text{H}$  shifts as frequency axes of PBMD was carried out and is shown in Figure 6. The carbon shifts are correlated to the known assignments of proton shieldings and clearly revealed the assignment of peaks in  $^{13}\text{C}$  NMR spectrum of PBMD as follows. Chemical shift:  $\delta$  (ppm) = 35.2371, 35.3297 ( $C_v$ ), 49.3681 ( $C_n$ ), 63.1594 ( $C_l$ ), 67.0208 ( $C_x$ ), 128.265, 128.436, 128.584, 135.228 ( $C_y$ ). The three group of peaks of 168.520, 168.587; 169.405, 169.433; and 170.200, 170.281, 170.313, 170.379 are in the chemical shift range of the carbonyl group. The definite assignment of them cannot be determined from the two-dimensional carbon–proton correlation, because the carbonyl carbon has no proton atom.

With these data, the carbon atoms bearing protons in the B unit of the copolymer are easily assigned and marked with the same letters used by their congeners in the  $^{13}\text{C}$  NMR spectrum of PBMD. In contrast to the uncertainty of the carbonyl shifts assignment and their bad signal to noise ratio, all the carbon signals of methylene and methine in the copolymers show great sensitivity to the sequence effects (Figure 4). The carbonyl signals are no longer considered in the following sequence analysis.

It is well-known that the ring-opening polymerization of  $\epsilon$ -caprolactone and morpholine-2,5-dione derivatives in the melt with stannous octoate as catalyst proceeds exclusively by cleavage of the ester bond.<sup>24</sup> On the basis of this theory, the triads and diads present in Figure 7 can be distinguished.

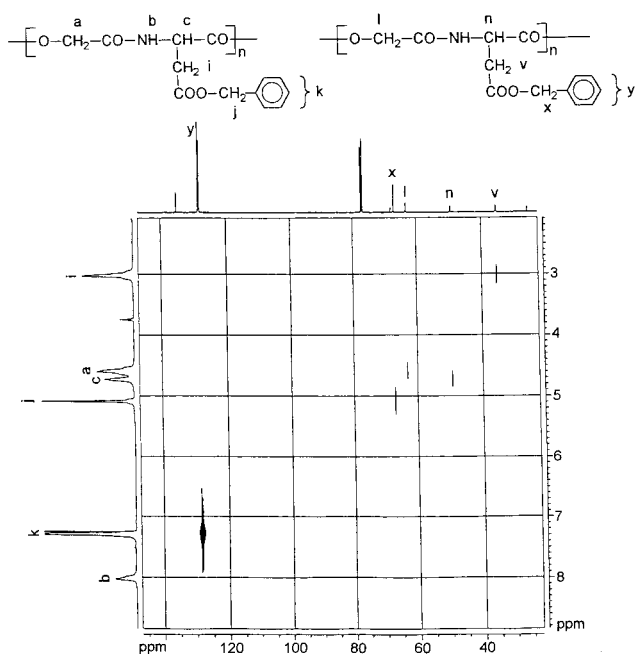


**Figure 6.** Two-dimensional carbon–proton correlation of PBMD ( $\text{CDCl}_3$ ).

The methylene carbon signals of  $r$ – $r''$ ,  $s$ – $s''$ ,  $t$ – $t''$  of the central  $\epsilon$ -oxycaproyl unit (C) in the sequences C–C–C, B–C–C, C–C–B, and B–C–B are assigned as follows. Peaks  $r$ ,  $s$ , and  $t$  can be assigned to the C–C–C sequence by comparison with the corresponding methylene carbon signals in PCL. Copolymers with a small mole fraction of BMD ( $X_B \leq 0.194$ ) show very weak signals for  $r''$ ,  $s''$ ,  $t''$ , and they can be assigned to the B–C–B sequence, which is very rare in these cases. Replacing a C unit by a B unit at the side of the carbonyl group will cause a larger upshift of these methylene carbons than the replacement at the other side of the central  $\epsilon$ -oxycaproyl unit (C). According to this, peaks  $r'$ ,  $s'$ ,  $t'$  and  $r''$ ,  $s''$ ,  $t''$  are assigned to the sequences of B–C–C and C–C–B, respectively. It is illustrated in Figure 7 that  $C_p$  and  $C_q$  only show diad sensitivity. Compared with the data from  $^{13}\text{C}$  NMR spectrum of PCL, peaks  $p$  and  $q$  are assigned to the C–C sequence. Furthermore, peaks  $p'$  and  $q'$  are assigned to the B–C sequence, because their signal intensities increase when  $X_B$  is raised.

When B is considered as the central unit, the methylene and methine signals of it show diad or triad sensitivity. Broad peak  $l$  does not appear when  $X_B \leq 0.194$ , and it increases greatly when  $X_B$  reaches 0.877. Obviously, it is assigned to the B–B sequence. Peak  $l'$  can be assigned to the C–B sequence, because it loses intensity when  $X_B$  is raised. With the same strategy stated above, peak  $n$  is assigned to the B–B sequence and  $n'$  is assigned to the B–C sequence. Extending the theory of  $C_l$  and  $C_n$  to  $C_v$ , peaks  $v$  and  $v'$  are assigned to B–B and B–C sequences, respectively, except that replacing a C unit by a B unit would cause a upshift in this case.

Unexpectedly,  $C_x$  also show sensitivity to sequence effects. But there are two group of peaks in the range of its chemical shift: 65.5959–65.8058 ppm; 66.8383–67.1789 ppm. Considering their chemical structure, copolymers may form a hydrogen bond which gives the B unit in the copolymer a much more stable conformation. And this tendency will be raised when

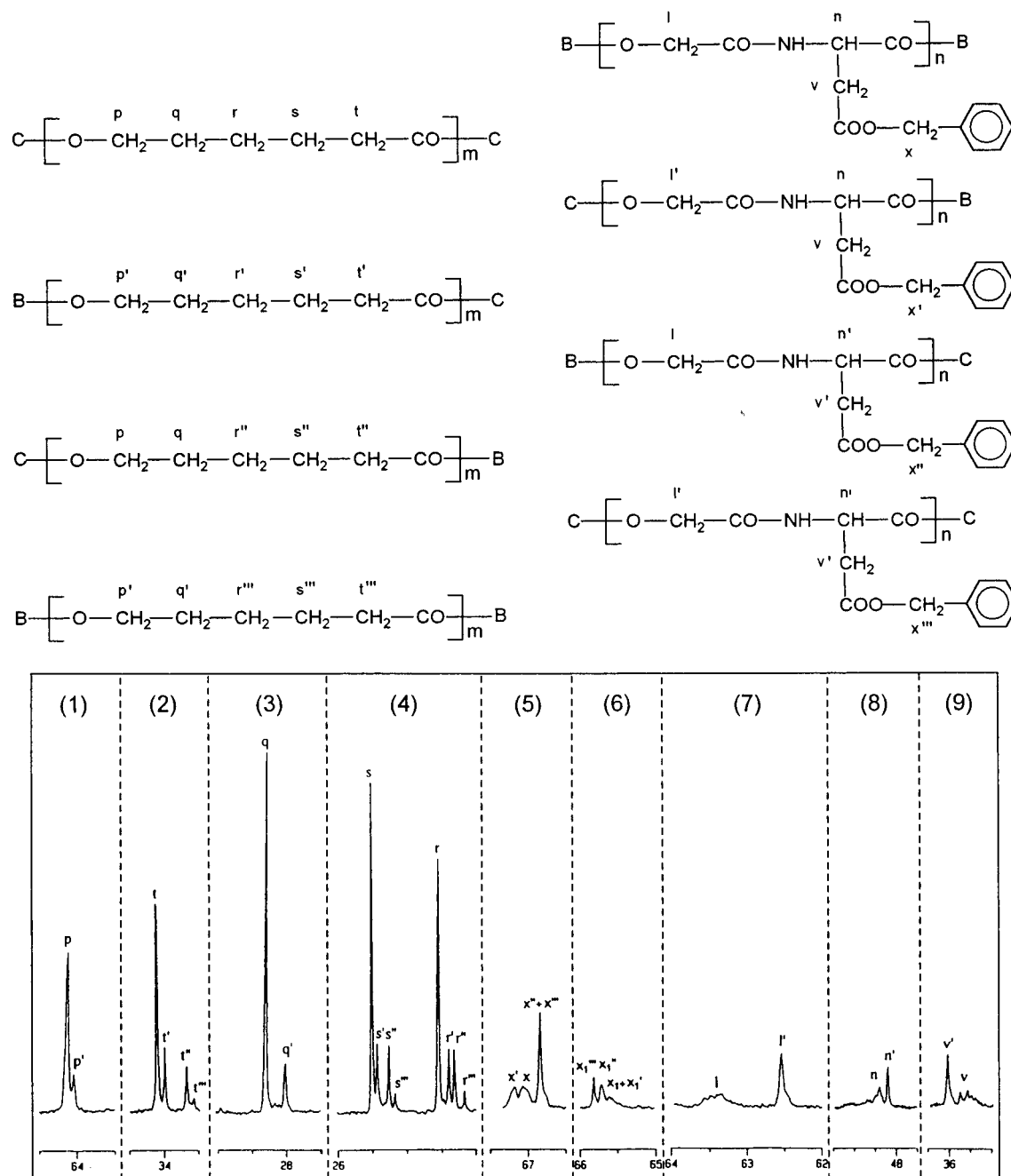


**Figure 7.** Expanded  $^{13}\text{C}$  NMR spectrum ( $\text{CDCl}_3$ ) of poly(CL-co-BMD) ( $X_B = 0.194$ , upper;  $X_B = 0.495$ , lower).

the number of B units present in the copolymers increases. On the basis of this hypothesis, the two group of peaks can be assigned to two types of B units which either have or have not formed a hydrogen bond. This idea is supported by the FTIR spectrum of the copolymer (Figure 8). The N-H stretch, which comes at  $3318\text{ cm}^{-1}$  in the spectrum, should belong to the copolymer which has a hydrogen bond formed in the sample. Those that have no hydrogen bond formed appear as a shoulder peak at  $3420\text{ cm}^{-1}$ .<sup>25</sup> In addition, the proton signals assigned to -NH- in the  $^1\text{H}$  NMR spectrum of poly(CL-co-BMD) move downfield from 7.1 to 8.0 ppm when  $X_B$  rises from 0.093 to 0.877, and this further proves the formation of a hydrogen bond inside the samples.

The intensity of peak group at 65.5959–65.8058 ppm decreases and that of the peak group at 66.8383–67.1789 ppm rises when  $X_B$  is increased. Considering

this phenomenon and the hypothesis stated above, the former peak group is assigned to those which have no hydrogen bond formed while the latter is assigned to those which contain a hydrogen bond in the B unit. Furthermore, each peak in this two group is distinguished with the method used for  $C_r$ ,  $C_s$ , and  $C_t$ . Peaks  $x, x', x'', x'''$  are assigned to the B-B-B, C-B-B, B-B-C, and C-B-C sequences, and peaks  $x_1, x_1', x_1'', x_1'''$  are assigned to the B-B-B, C-B-B, B-B-C, and C-B-C sequences.

When  $X_B$  is lower than 0.093, there are only peaks  $l', n', v', x''''$ , and  $x_1'''$ , which appear while the other peaks are absent, and this indicates the predominant existence of the sequences C-B, B-C, and C-B-C in this case.

The assignments of all the peaks in the  $^{13}\text{C}$  NMR spectrum of the copolymers are summarized in Table 2.

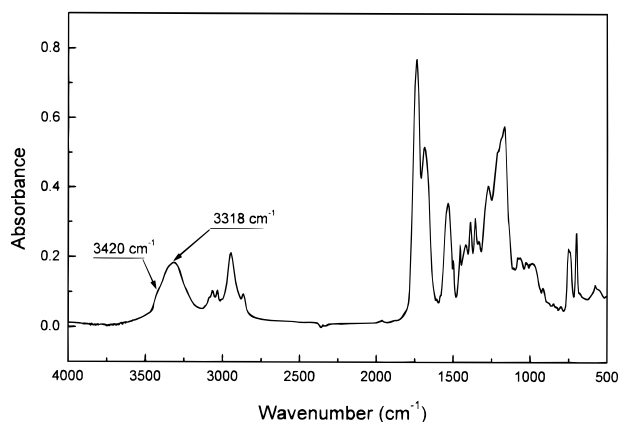


**Figure 8.** FTIR spectrum of poly(CL-co-BMD) ( $X_B = 0.495$ ).

**Table 2. Assignment of Peaks in  $^{13}\text{C}$  NMR Spectra ( $\text{CDCl}_3$ ) Used for Sequence Analysis of Poly(CL-co-BMD)**

carbon atoms	peaks assignment (ppm)
$\text{C}_r$	24.5378 (r); 24.3867 (r'); 24.2960 (r''); 24.1565 (r''')
$\text{C}_s$	25.4902 (s); 25.4128 (s'); 25.2462 (s''); 25.1485 (s''')
$\text{C}_t$	34.0789 (t); 33.9717 (t'); 33.6420 (t''); 33.5450 (t''')
$\text{C}_p$	64.1209 (p); 64.0307 (p')
$\text{C}_q$	28.2979 (q); 28.0064 (q')
$\text{C}_l$	63.3488 (l); 62.5315 (l')
$\text{C}_n$	48.3970 (n); 48.1878 (n')
$\text{C}_v$	35.5863 (v); 36.0794 (v')
$\text{C}_x$	67.0625 (x); 67.1789 (x'); 66.8383 (x''+x'''); 65.5959 (x1 + x1'); 65.7005 (x1''); 65.8058 (x1''')

**Table 3. Average Length of C Blocks ( $L_C$ )**

carbon atom	$L_C$ of no. 1 <sup>a</sup>	$L_C$ of no. 2 <sup>a</sup>	$L_C$ of no. 3 <sup>a</sup>	$L_C$ of no. 4 <sup>a</sup>	$L_C$ of no. 5 <sup>a</sup>
$\text{C}_p$	4.86	4.29	1.98	1.55	1.00
$\text{C}_q$	8.79	5.02	1.94	1.54	1.12
$\text{C}_r$	9.00	4.34	2.08	1.59	1.10
$\text{C}_s$	9.85	4.21	1.98	1.58	1.19
$\text{C}_t$	10.56	4.95	2.11	1.62	1.03
$\bar{L}_c^b$	9.55	4.56	2.01	1.58	1.09

<sup>a</sup> Here, no. 1–no. 5 refer to the samples listed in Table 1. <sup>b</sup>  $\bar{L}_c$  refers to the average of  $L_C$ .

The average lengths of homogenous C block ( $L_C$ ) and B block ( $L_B$ ) are calculated with the following equations:<sup>22</sup>

$$L_C = \frac{I_r + I_{r'}}{I_{r''} + I_{r'''}} + 1 = \frac{I_s + I_{s'}}{I_{s''} + I_{s'''}} + 1 = \frac{I_t + I_{t'}}{I_{t''} + I_{t'''}} + 1 = \frac{I_p}{I_{p'}} + 1 = \frac{I_p}{I_{p'} + 1} \quad (1)$$

$$L_B = \frac{I_x + I_{x'} + I_{x_1} + I_{x_1'}}{I_{x''} + I_{x'''} + I_{x_1''} + I_{x_1'''}} + 1 = \frac{I_n}{I_{n'}} + 1 = \frac{I_v}{I_{v'}} + 1 = \frac{I_l}{I_{l'}} + 1 \quad (2)$$

$I$  represents the peak intensity. The results of the average lengths are shown in Tables 3 and 4.

It is found in Table 3 that  $L_C$  of sample 1 calculated from peaks p and p' has a much larger error. This is attributed to the overlap of these two peaks which would cause an incorrect integral ratio. In Table 4,  $L_B$  of sample 4 cannot be calculated from peaks n and n', because they are joined, resulting in a broad peak which is difficult to distinguish.

**Table 4. Average Length of B blocks ( $L_B$ )**

carbon atom	$L_B$ of no. 1 <sup>a</sup>	$L_B$ of no. 2 <sup>a</sup>	$L_B$ of no. 3 <sup>a</sup>	$L_B$ of no. 4 <sup>a</sup>	$L_B$ of no. 5 <sup>a</sup>
$\text{C}_v$	1.00	1.00	1.96	4.17	8.75
$\text{C}_n$	1.00	1.00	2.24		8.93
$\text{C}_l$	1.00	1.00	1.97	4.07	9.02
$\text{C}_x$	1.00	1.12	1.98	3.58	6.73
$\bar{L}_B^b$	1.00	1.03	2.04	3.94	8.36

<sup>a</sup> Here, no. 1–no. 5 refer to the samples listed in Table 1. <sup>b</sup>  $\bar{L}_B$  refers to the average of  $L_B$ .

**Table 5. Comparison of the Mole Fraction of the B Unit in Poly(CL-co-BMD) ( $X_B$ ) Obtained from Different Sources**

$X_B$	no. 1 <sup>a</sup>	no. 2 <sup>a</sup>	no. 3 <sup>a</sup>	no. 4 <sup>a</sup>	no. 5 <sup>a</sup>
$X_B$ from eq 3	0.095	0.184	0.504	0.714	0.885
$X_B$ from $^1\text{H}$ NMR	0.093	0.194	0.517	0.753	0.877

<sup>a</sup> Here, no. 1–no. 5 refer to the samples listed in Table 1.

**Table 6. Results of Copolymerization of  $\epsilon$ -caprolactone and BMD for Different Reaction Times<sup>a</sup>**

sample no.	$x_B^b$	$X_B^b$	$\bar{L}_C^c$	$\bar{L}_B^c$	% convn CL BMD	amt of catalyst ( $\mu\text{L}$ )	$t$ (min)
6	0.480	0.815	9.70	11.7	32.9	11.1	60
7	0.485	0.800	1.72	4.22	12.0	79.3	90
8	0.452	0.697	1.53	3.99	22.3	80.9	140
9	0.477	0.676	1.76	3.32	27.0	82.4	190
3	0.517	0.495	2.01	2.04	95.0	95.5	250

<sup>a</sup>  $x_B \approx 0.5$ ; mole ratio monomer/catalyst = 1000/1. <sup>b</sup>  $x_B$  is the mole fraction of BMD in feed;  $X_B$  is the mole fraction of BMD in copolymer. <sup>c</sup>  $\bar{L}_C$ ,  $\bar{L}_B$ , and conversion of monomers are calculated from the data of  $^1\text{H}$  NMR spectrum ( $\text{CDCl}_3$ ). <sup>d</sup>  $\bar{L}_C$  and  $\bar{L}_B$  are obtained from the interpretation of  $^{13}\text{C}$  NMR spectrum ( $\text{CDCl}_3$ ).

On the basis of these data, the mole fraction of BMD in the copolymer ( $X_B$ ) can also be calculated from

$$X_B = \frac{L_B}{L_B + L_C} \quad (3)$$

As shown in Table 5, the  $X_B$  values obtained from eq 3 are in good agreement with the  $X_B$  values calculated from  $^1\text{H}$  NMR spectrum. This result further confirms the interpretation of the  $^{13}\text{C}$  NMR spectra of poly(CL-co-BMD).

Considering the data from Table 3 and Table 4, the copolymer is composed of an  $\epsilon$ -oxycaproyl block subdivided by a single depsipeptide unit (or B unit) when  $X_B$  is lower than 0.194. When  $X_B$  reaches 0.495, the composition of the copolymer turns into a random sequence distribution. On the other aspect, this also happens to depsipeptide block (or B block) when  $X_B$  is lowered from 0.877 to 0.495. This type of sequence distribution is the result of severe transesterification taking place during the reaction at 152 °C.

To further clarify the process in which these polymer sequences are obtained, copolymerization samples ( $x_B \approx 0.5$ ) with different reaction times are studied, and the results are listed in Table 6. Unexpectedly, the data shows that BMD polymerizes much faster than CL. The conversion of BMD quickly reach 80% while the conversion of CL keep at 10–30% until the jump at the end of the copolymerization.  $\bar{L}_B$  decreases from 9.70 to 2.04 and  $\bar{L}_C$  increases from about 1 to 2.01, while the reaction time is raised from 60 to 250 min. This change of the sequence further confirms that the transesterification which happens in the polymerization process greatly

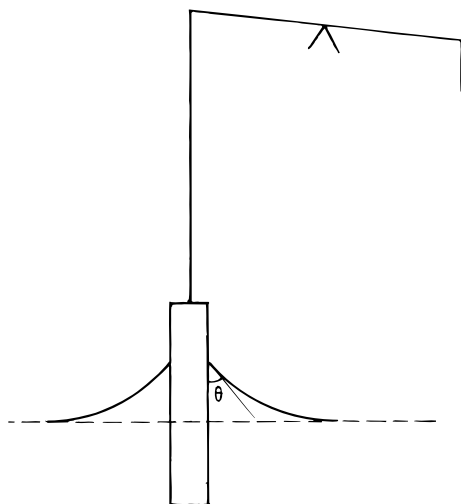


**Figure 9.** Schematic diagram of the Wilhelmy plate experiment.

affected the sequence distribution of the copolymers. An Italian group<sup>26</sup> had reported a similar result. They stated in their paper that when L-lactide and  $\epsilon$ -caprolactone were copolymerized, the polymerization rate of L-lactide was higher than that of  $\epsilon$ -caprolactone.

#### Hydrophilicity of the Deprotected Copolymers.

In order to study the hydrophilicity of the resulting deprotected copolymers with different monomer mole fractions in the feed, the dynamic contacting angles (DCA) for them were determined in distilled water at 37 °C.

In fact, the dynamic contacting angle analyzer (DCA-322) is designed on the basis of the Wilhelmy plate experiment.<sup>27</sup> The schematic diagram of this apparatus is shown in Figure 9.

Suppose the Wilhelmy plate is allowed to dip beneath the horizontal water surface; then the weight of the meniscus ( $w$ ) is given by

$$w = \gamma P(\cos \theta) - w' = \gamma P(\cos \theta) - kd \quad (4)$$

It is decreased by a term  $w'$ , the buoyant force on the submerged plate. The latter is proportional to the depth of immersion  $d$ .  $k$  is a suitable proportionality constant.  $P$  is the circumference of the plate. When the experiment is carried out under set conditions, the surface tension  $\gamma$  of distilled water is also a constant. Once  $w$  and  $d$  are known, the contact angle  $\theta$  can be calculated from eq 4 easily. In the measuring process, the dynamic contacting angle analyzer collects data for  $w$  and  $d$  in the immersion–emersion process of the plate, and it gives a curve like that shown in Figure 10 ( $X_B = 0.093$ , deprotected). In the immersion process,  $w$  is gradually reduced with an increase in  $d$ , while this is reversed in the emersion process. The least-squares method is used by the dynamic contacting angle analyzer to analyze the data in a selected region and gives the advancing angle (contacting angle in immersion) and the receding angle (contacting angle in emersion). These angles are defined as dynamic contacting angles, which reflect the hydrophilicity of the plate surface or the substance coated on the plate. The smaller the dynamic contacting angle, the more hydrophilic the surface is.

In the testing process, some deprotected copolymer coated on the glass was washed down by water, and this was much more severe for sample no. 5, which is more hydrophilic than those of sample nos. 1–4. In order to

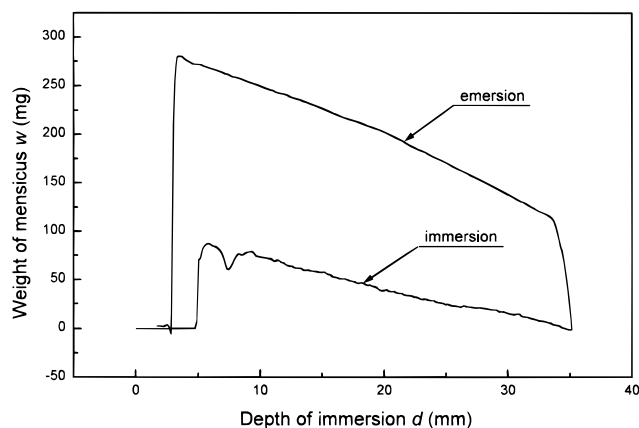


**Figure 10.** DCA result (cycle I) of deprotected copolymer ( $X_B = 0.093$ ).

**Table 7. Advancing Angles (deg) of Copolymers (Cycle I)**

	no. 1 <sup>a</sup>	no. 5 <sup>a</sup>
protected copolymers	76.728	76.937
deprotected copolymers	76.125	49.19

<sup>a</sup> Here, no. 1 and no. 5 refer to the samples listed in Table 1.

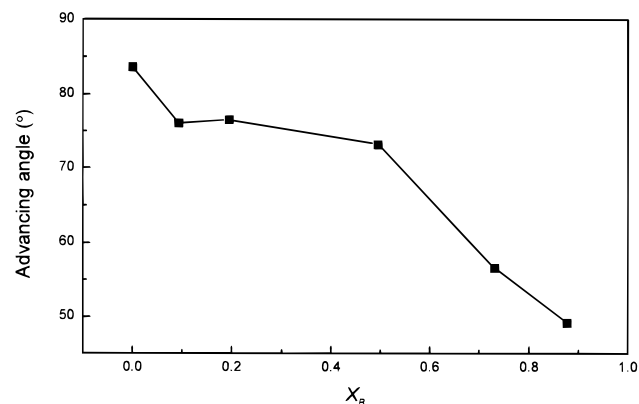


**Figure 11.** Advancing angle in cycle I of deprotected copolymers.

get rid of the errors caused by this phenomenon, the DCA data of cycle II and data of the receding angle in cycle I are kept out of consideration.

The advancing angles in cycle I of both the protected and the deprotected copolymers of samples no. 1 and no. 5 are shown in Table 7. It reveals that the deprotection processes bring very little change in hydrophilicity to sample no. 1, while the hydrophilicity of sample no. 5 is greatly increased after the deprotection process. This difference is surely attributed to the relatively abundant liberated carboxylic acid group that existed in the deprotected sample no. 5.

The result of advancing angle in cycle I of all the deprotected copolymers is illustrated in Figure 11. It is clearly shown that the more BMD monomer is added, the smaller the advancing angle is obtained, which indicates a higher hydrophilicity of the copolymer. Careful consideration of Figure 11 shows that the advancing angle of the deprotected copolymer has a sharp drop when  $X_B$  is adjusted from 0 to 0.093. It remained almost constant until the turning point of 0.495, where it moves into another deep drop to 49.19° corresponding to the highest content of BMD ( $X_B = 0.877$ ).

Because of the increase in  $X_B$ , it may be suggested that the hydrophilicity of the deprotected copolymer

should keep a linear relation with  $X_B$ . However, the results shown in Figure 11 clearly indicate a more complex mechanism beyond the prediction. In fact, these data for advancing angles reflect the hydrophilicity of the deprotected copolymer coated on the glass, which is mainly related to the surface composition of the copolymers. Correlation of Figure 11 with the data of  $L_C$  and  $L_B$  obtained in sequence analysis suggests that the long hydrophobic  $\epsilon$ -oxycaproyl block may have a so called "package effect" to the hydrophilic depsipeptide unit which prevents it from contact with the environment. This effect lasts till the turning point of  $X_B = 0.495$  where  $L_C \approx L_B \approx 2$ ; the independent phase of the depsipeptide block starts to emerge and to form a much more hydrophilic polymer surface on the testing plate. On the basis of this analysis, two suggestions are put forward:

(i) To obtain polyesteramide materials with limited hydrophilicity, a morpholine-2,5-dione derivative with hydrophilic pendant functional group can be copolymerized with lactone in a wide range of mole fractions in the feed, and it may leave enough space for the adjustment of the degradability of the copolymer, which relates to the mole fraction of comonomers.

(ii) In the process of producing a delivery system for water soluble drugs, a polyesteramide with pendant hydrophilic functional group should be deposited onto the surface of the drug gradually to prevent the package effect, which can interfere with perfect encapsulation and the desired release rate of the drug.

## Conclusions

The monomer (3*S*)-3-[(benzyloxycarbonyl)methyl]-morpholine-2,5-dione (BMD) has been successfully copolymerized with  $\epsilon$ -caprolactone at wide range of mole fractions in the feed. The average molecular weight of the copolymer decreases as the mole fraction in feed of BMD ( $X_B$ ) increases. The deprotection method using Pd/C as catalyst is proved to be effective, but it may lead to slight main-chain cleavage.

The  $^{13}\text{C}$  NMR interpretation and the sequence analysis of the copolymers show that the copolymer is composed of a  $\epsilon$ -oxycaproyl block subdivided by a single depsipeptide unit (or B unit) when  $X_B$  is lower than 0.194. When  $X_B$  reaches 0.495, the composition of the copolymer turns into a random sequence distribution. On the other hand, this also happens to the depsipeptide block (or B block) when  $X_B$  is lowered from 0.877 to 0.495. This phenomenon is attributed to the severe transesterification reaction which happened during the polymerization processes.

Sequence analysis of the copolymers (BMD/CL  $\approx$  1/1) with different reaction time shows that the newly synthesized monomer polymerizes much faster than  $\epsilon$ -caprolactone.

The hydrophilicity of both protected and deprotected copolymers has been carefully investigated with DCA

measurement. The change in hydrophilicity as illustrated in Figure 11 is well explained on the basis of the sequence analysis of the copolymers.

**Acknowledgment.** The authors are indebted to Dr. G. Y. Wei of Polymers & Colloids, Cavendish Laboratory of Cambridge University, Cambridge, England, for valuable discussions and his critical reading of the manuscript.

## References and Notes

- (1) Vert, M. *Angew. Makromol. Chem.* **1989**, 166/167, 155.
- (2) Feng, X. D.; Song, C. X.; Chen, W. Y. *J. Polym. Sci.: Polym. Lett. Ed.* **1983**, 21, 593.
- (3) Song, C. X.; Feng, X. D. *Macromolecules* **1984**, 17, 2764.
- (4) Song, C. X.; Sun, H. F.; Feng, X. D. *Polym. J.* **1987**, 19, 485.
- (5) Blanco-Prieto, M. J.; Fattal, E.; Gulik, A.; Dedieu, J. C.; Roques, B. P.; Couvreur, P. *J. Controlled Release* **1997**, 43, 81.
- (6) Rafati, H.; Coombes, A. G. A.; Adler, J.; Holland, J.; Davis, S. S. *J. Controlled Release* **1997**, 43, 89.
- (7) Braud, C.; Vert, M. *Polym. Prepr. (Am. Chem. Soc., Div. Polym. Chem.)* **1985**, 24 (I), 71.
- (8) Arnold, S. C.; Lenz, R. W. *Makromol. Chem., Makromol. Symp.* **1986**, 6, 285.
- (9) Kimura, Y.; Shirotani, K.; Yamane, H.; Kitao, T. *Macromolecules* **1988**, 21, 3338.
- (10) Ouchi, T.; Fujino, A. *Makromol. Chem.* **1989**, 190, 1523.
- (11) Zhou, Q. X.; Kohn, J. *Macromolecules* **1990**, 23, 3399.
- (12) Fietier, I.; Le Borgne, A.; Spassky, N. *Polym. Bull. (Berlin)* **1990**, 24, 349.
- (13) in't Veld, P. J. A.; Dijkstra, P. J.; Feijen, J. *Makromol. Chem.* **1992**, 193, 2713.
- (14) Barrera, D. A.; Zylstre, E.; Lansbury, P. T.; Langer, R. *Macromolecules* **1995**, 28, 425.
- (15) Hrkach, J. S.; Ou, J.; Lotan, N.; Langer, R. *ACS Symposium Series 627*; American Chemical Society: Washington, DC, 1996; p 93.
- (16) Ouchi, T.; Shiratani, M.; Jinno, M.; Hirao, M.; Ohya, Y. *Makromol. Chem., Rapid Commun.* **1993**, 14, 825.
- (17) Ouchi, T.; Nozaki, T.; Okamoto, Y.; Shiratani, M.; Ohya, Y. *Makromol. Chem. Phys.* **1996**, 197, 1823.
- (18) Wang, D.; Feng, X. D. *Macromolecules* **1997**, 30, 5688.
- (19) Vert, M.; Lenz, R. W. *Polym. Prepr. (Am. Chem. Soc., Div. Polym. Chem.)* **1979**, 20, 608.
- (20) Kricheldorf, H. R.; Mang, T.; Jonte, J. M. *Makromol. Chem.* **1985**, 186, 955.
- (21) Kricheldorf, H. R.; Coutin, B.; Sekiguchi, H. *J. Polym. Sci.: Polym. Chem. Ed.* **1982**, 20, 2353.
- (22) in't Veld, P. J. A.; Ye, W. P.; Klap, R.; Dijkstra, P. J.; Feijen, J. *Makromol. Chem.* **1992**, 193, 1927.
- (23) Shen, Z. Q.; Chen, X. H.; Shen, Y. Q.; Zhang, Y. F. *J. Polym. Sci., Part A: Polym. Chem.* **1994**, 32, 597.
- (24) in't Veld, P. J. A.; Dijkstra, P. J.; van Lochem, J. H.; Feijen, J. *Makromol. Chem.* **1990**, 191, 1813.
- (25) Wang, Z. X. In *Modern Technology and Application of FTIR Spectrum*, 1st ed.; Wu, J. G., Ed.; Publishing House of Scientific and Technical Document: Beijing, 1992; Vol. 1, p 623 (in Chinese).
- (26) Pergeo, G.; Vercellio, T.; Balbontin, G. *Makromol. Chem.* **1993**, 194, 2463.
- (27) Hiemenz, P. C. *Principles of Colloid and Surface Chemistry*, 2nd ed; Marcel Dekker, Inc.: New York, 1986; p 317.

MA971446B